PROCESS MODELING AND MANUFACTURING OF THERMOPLASTIC PREPREG TAPE

Alex M. Reichanadter[1,2], Joshua S. Dustin[2], Jan-Anders E. Mansson[1,2]

[1]Davidson school of Chemical Engineering. Purdue University
480 West Stadium Avenue
West Lafayette, Indiana/USA

[2]Composites Manufacturing and Simulation Center (CMSC)
1105 Challenger Avenue
West Lafayette, Indiana/USA

ABSTRACT

In order to meet new fuel efficiency and recyclability criteria, thermoplastic composites are finding more applications in automobiles. The demand from the transportation industry is expected to help grow the global thermoplastic composites market from $26.16 billion in 2017 to $67.87 billion by 2026 [1]. Thermoplastic composite parts are often manufactured from pre-impregnated (prepreg) tape or organo sheets in order to reduce cycle times. This approach divides the thermoplastic composite part manufacturing into two distinct steps, an initial impregnation step where resin saturates the fiber bed and a final thermoforming step to take on the part shape. In this supply chain, the production of thermoplastic tape is a bottleneck for manufacturing. In order to address this issue, we at the Composites Manufacturing & Simulation Center (CMSC), have built a custom thermoplastic prepreg line in order to study the challenges associated with increased throughput. Our prepreg line is configurable for traditional thermoplastic hot-melt impregnation, fiber co-mingling, and film impregnation. In addition to the flexible line configuration, process models will be developed to predict line tape quality and later used to guide the design and operation of future prepreg tape lines.

1. INTRODUCTION

Lightweight composite materials are attractive to industries where strength–to–weight ratio is important. The aerospace industry has long been the most notable for incorporating composite materials in their products [2]. In this industry, high costs and low cycle times were accepted because cost savings from weight reduction and long part design lifecycle outpaced the expenses generated from low production volume. Furthermore, an aerospace part design will remain the same for decades because of the lengthy FAA certification process [3]. Until recently, composite material was primarily consumed by the aerospace industry. However, new industries are embracing lightweight composite material, which do not conform to previous norms. Most prominently, the automotive industry is seeking to utilize composite components in their design, creating new demands on the composites industry such as production volume, improved cycle times, material flexibility, cost, and low tack at room temperature [4].

SAMPE Conference Proceedings. Charlotte, NC, May 20-23, 2019. Society for the Advancement of Material and Process Engineering – North America.

Pre-impregnated composite (prepreg) is an intermediate material used to construct complex, structural composite parts. Since the 1960's, the aerospace industry has replaced metal parts with an equivalent composite analog in an effort to increase performance (strength, stiffness, or specific energy absorption) and decrease weight [2]. Currently, the automotive industry is adopting composite material in order to meet new fuel economy ratings and emissions targets imposed by the US government [5]. Composites produced from prepreg are appealing to the automotive industry to meet desired strength/stiffness/energy absorption to weight ratios that lead to acceptable improvements in fuel efficiency.

Traditionally, prepreg parts are typically laid up by hand, therefore, exceeding the cycle times needed for the automotive industry. Thus a new manufacturing technique was needed to merge the structural performance achieved by prepreg layup and cycle times from discontinuous fiber molding processes like sheet molding compounds (SMCs), which are currently being used on vehicles like the 2016 Jeep Wrangler [6]. Prepreg platelet molding compounds (PPMCs) appear to be a promising manufacturing process that can achieve structural performance and maintain cycle times suitable for the automotive industry [7]. Further, existing metal stamping presses could be repurposed for this material form at little capital investment.

2. PREPREG LINE OPERATION

The prepregging process involves the flow of resin through a fiber bed. The physics governing fiber bed impregnation are captured by Darcy's Law. This relates the permeability (K), bed thickness (X), viscosity (η), fiber volume fraction (V_f) and pressure (ΔP) to the superficial velocity at which material flows through a porous medium. The differential form of Darcy's law is shown in Equation 1 [8]. This simplified model is applicable when the flow regime has a Reynolds number < 1, which are typical conditions during the prepregging process. For aligned fiber beds, the permeability is inversely related to the applied pressure, as studied extensively by Gutowski, Advani, and Dave [9-11]. Prior to impregnation, fiber bed thickness is controlled by spreading fiber tows. Production lines are designed to take advantage of unique properties of the matrix material (viscosity, physical state at room temperature, etc.) to minimize processing time.

$$\frac{dX}{dt} = \frac{K\Delta P}{\eta X\,(1-V_f)} \qquad [1]$$

The goal of impregnation is to saturate the fiber bed with polymer matrix while minimizing porosity. Composite mechanical properties are inversely related to void fraction [12]. Thus, minimum void content in the final composite part is desired (aerospace rule of thumb is below 1 volume %). Unfortunately, void formation occurs during the impregnation of the fiber bed due to incomplete impregnation or poor wetting of the fibers [13]. Grunenfelder et al. showed void content in the final laminate part is highly dependent on the quality of prepreg used [14]. Barrera-Betanzos, Gabrion, Advani, and Gangloff Jr support this observation finding pressure and temperature have little effect on removing voids from a composite part. Instead, the resin saturation of the prepreg greatly influences void removal [15-18].

2.1 Prepregging Methods

Examples of processes exploiting different aspects of Darcy's Law include: hot-melt (S-wrapped or nip-rolled), fiber co-mingling, film stacking, solution processing, emulsification, and powder

impregnation [19]. Research groups choose a manufacturing approach for the ease, simplicity, relevance to industry, or low equipment cost. Common prepreg manufacturing approaches in academic institutions are pultrusion, fiber co-mingling, film stacking, and hot-melt. Modeling and optimizing these existing processes rather than designing manufacturing flexibility is the focus of current research [14, 15, 18, 20-26]. As the composites industry evolves, new technologies are being desired for prepreg lines capable of easily switching between thermoset and thermoplastic prepreg production [4, 27].

Of these approaches, the focus is on reducing the distance that the matrix must flow. We will discuss 3 such approaches here. 1) Film stacking is a simple method where films of matrix material and beds of fiber are alternated to reduce impregnation distance. This approach is compatible with thermoset and thermoplastic, but requires additional processing steps [28-30]. In addition, 2) thermoplastic fibers can be commingled with reinforcing fibers to reduce impregnation distances. 3) Powder deposition also seeks to reduce flow distances by using a fluidized bed of thermoplastic powder to disperse the powder through the thickness. Routes 2 and 3 are inaccessible to most thermosets because they are a liquid at room temperature [24, 25, 31].

The pultrusion and hot-melt processes are attractive for their higher throughput and simplicity, but are restricted to processing lower viscosity resins [20-23]. Reducing a material's viscosity by dissolving the matrix in a solvent is possible [24, 25, 32, 33], but this introduces environmental concerns or reduces matrix performance [23]. Thus these processes are typically compatible with thermoset polymers rather than thermoplastic. Emulsification aims to avoid these issues. However, this technique requires additional processing to remove the solvent and reduce void content as shown by Ramani, Diez-Pascual, Fang, and Sorrentino [19, 28, 29, 34-36].

2.2 Prepreg Quality and Characterization for Modeling

The glass transition temperature and resin saturation are two ways that we will use to evaluate prepreg quality, and the glass transition temperature (T_g) is a measure of the long range chain mobility. Analytically, the glass transition temperature can be defined thermodynamically as the observed change in the volume vs temperature slope [37]. Resin saturation can be determined by taking micrograph cross-sections and examining them under a microscope. Evaluating prepreg quality with these two factors is accomplished by:

- For reacting systems (thermosets), an initial glass transition temperature (T_{go}) and final glass transition temperature ($T_{g\infty}$) are needed to describe the polymer system. From this information, the degree of cure advancement can be estimated for the system to determine if the matrix material still has the desired processing window for subsequent process steps [37, 38].

- While for non-reacting systems (thermoplastics) the T_g can be used to infer if thermal degradation of the material has occurred resulting in out of spec performance. In order to determine the glass transition temperature for these systems, a full rheo-kinetic characterization needs to be performed to assess the quality of the resulting prepreg material.

- Resin saturation is another way to gauge the "as-designed" performance to the "as-manufactured" expectations of the prepreg based on cross-sections of prepreg. These cross-sections can be examined under microscope to determine void content and used to estimate final part, "as-manufactured" performance.

2.3 Fiber Bed Behavior

During a general prepregging operation, mechanical pressure is applied to encourage the flow of molten matrix material to flow through the fiber bed. This pressure causes the fiber bed to compact, increasing the fiber volume fraction while reducing the inter-fiber spacing. The reduction in inter-fiber spacing corresponds to a reduction in permeability of the fiber bed. There have been many experimental and theoretical characterization approaches to relate fiber volume fraction to the permeability and/or pressure for aligned fibers.

When flowing material through the fiber bed, the fiber volume fraction (V_f) is proportional to the driving force (pressure) that is applied. Understanding the fiber volume fraction has implications on flow and resulting tape quality. Typically, the fiber volume fraction is approximated using the model suggested by Gutowski, Equation 2. This is an empirical model which was originally developed to explain fiber bed compaction behavior in laminates. The V_a term refers to the fiber volume fraction where the fiber bed locks and fibers are incapable of further compaction. The V_o term refers to the fiber volume fraction at which a finite load can be supported. The A term is effectively the fiber bed's modulus [9]. However, all of these terms are empirically determined and are loosely tied to the definitions provided previously [39].

$$\Delta P = A \frac{\sqrt{\frac{V_f}{V_o}} - 1}{\left(\sqrt{\frac{V_a}{V_f}} - 1\right)^4} \quad [2]$$

This relationship between pressure and volume fraction is important to the prepregging process. Increasing the fiber volume fraction decreases fiber spacing, which restricts the ability for material to flow through the fiber bed and can result in particle filtration after a critical fiber spacing has been achieved. Since the fiber volume fraction is changing throughout the infusion step, the permeability (K) will change, as well. The Carmen-Kozeny Equation 3 has been shown to estimate the fiber bed permeability across most fiber volume fractions. This permeability relationship was first derived for porous beds of aligned cylinders with a uniform radius (r_f) [8, 40, 41].

$$K = \frac{r_f^2 (1 - V_f)^3}{4 k_{ii} V_f^2} \quad [3]$$

2.3 S-Wrap Impregnation Route for Hot-Melt

A simplification of the S-Wrap process is shown in Figure 1. In this process, tensioned fibers are pulled over rollers. The tension serves two purposes 1) maintain fiber alignment and 2) generate pressure as the sandwich structure passes over the rollers. These rollers can be static, idle, or driven. Static rollers will generate greater pressure for impregnation, but greater tension will be generated in the fibers. The tension could reach a critical value where fibers begin breaking

resulting in “fuzz balls” or other defects forming along the prepreg. Additionally, the friction within the system may become too great and exceed the pulling force capacity of the line. Static pins can suffer from running dry. Where the resin film has been depleted and the fibers begin to rub on the pins. This results in similar fiber breakage. Idle rollers may also increase the friction in the system, however the increased friction is less than the static rollers. As such, the risk of exceeding the available pulling force is reduced. The likelihood of fiber breakage is also mitigated. Like the idle rollers, driven rollers further reduce the probability of fiber breakage. These rollers can match the line speed of the process which will result in negligible pulling force increases.

In comparison, the tension with idle and driven rollers is nearly uniform across the process while static rollers continue to build tension in the line. Consistent tension throughout the process eases the operation of the line as line speed will not influence the tension. This provides a simple relationship between resin saturation and line speed/initial tension. However, with static rollers, the tension is a function of the line speed. This variability in tension will alter the pressure over each roller. Now there is a risk of locking the fiber bed such that transverse flow of resin is not possible. The point at which flow is not possible can be predicted from the Carmen-Kozeny equation.

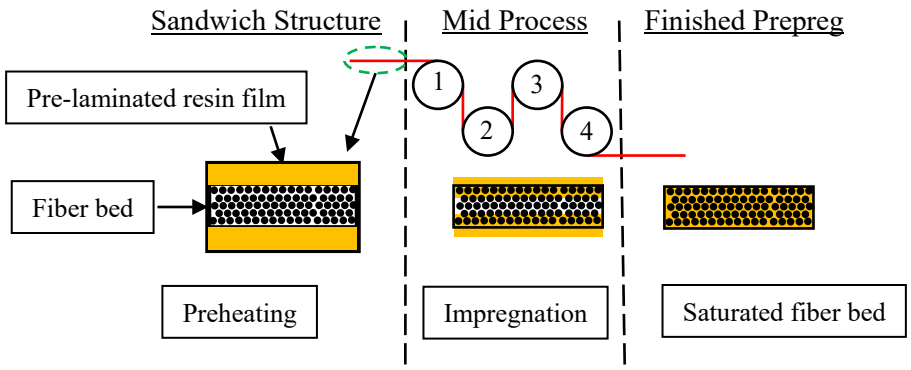

Figure 1: Simplified S-Wrap impregnation process where tension over rollers are the driving force for impregnation. Numbers correspond to peaks in Figure 4.

In addition to the tension, the angle of wrap around the roller are important to the development of the pressure to drive the resin into the fiber bed. For this example, we will consider rollers to be frictionless thus the tension remains constant throughout the process. The wrap angle depends on the diameter and position of adjacent rollers and the point where the fiber becomes tangent to the roller. This information can be used to determine the wrap angle of the fiber on the roller. Geometrically, two circles can have up to four unique tangent lines (two inner and two outer). The “inner” tangents are of interest to this process as the fiber bed will leave the top of the first roller and begin contact at the bottom of the next roller. Both wrapping options are represented geometrically in Figure 2.

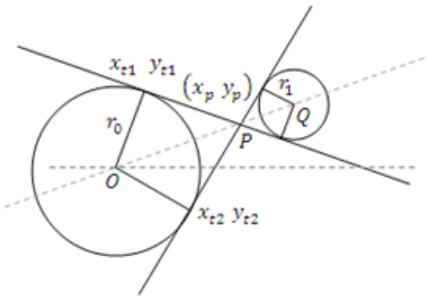

Figure 2: Representation of inner tangents between two circles [42].

With only the relative position and radius of adjacent rollers, the tangent line and point where contact is made/lost with the rollers can be determined with geometry. The following will discuss the geometry used to identify these important points. The point where the two inner tangents cross will be referred to as P (X_p, Y_p), which are defined in Equations 4 and 5. Identifying these points simplifies the subsequent calculations for the tangent points. The values a_i and b_i represent the X and Y centers, respectively for the i^{th} cylinder. The X and Y points for the 1st cylinder (#0) are represented in Equations 6 and 7, respectively. It is important to note the equations are similar, but the order of the +/- is switched between the two and corresponds to the 1st/2nd tangent point (there are two inner tangents). For the case where the fibers are going from the top of the 1st cylinder to the bottom of the next, Equation 6 would use the negative sign and Equation 8 would have a positive sign. The same process is repeated for the next roller, shown in Equations 8 and 9 [42].

$$X_p = \frac{a_1 r_0 + a_0 r_1}{r_0 + r_1} \quad [4]$$

$$Y_p = \frac{b_1 r_0 + b_0 r_1}{r_0 + r_1} \quad [5]$$

$$X_{t0,1}^{+} = X_{t0,2}^{-} = \frac{r_0^2 (X_p - a_0) \pm r_0 (Y_p - b_0) \sqrt{(X_p - a_0)^2 + (Y_p - b_0)^2 - r_0^2}}{(X_p - a_0)^2 + (Y_p - b_0)^2} + a_0 \quad [6]$$

$$Y_{t0,1}^{-} = Y_{t0,2}^{+} = \frac{r_0^2 (Y_p - b_0) \mp r_0 (X_p - a_0) \sqrt{(X_p - a_0)^2 + (Y_p - b_0)^2 - r_0^2}}{(X_p - a_0)^2 + (Y_p - b_0)^2} + b_0 \quad [7]$$

$$X_{t1,1}^{+} = X_{t1,2}^{-} = \frac{r_1^2 (X_p - a_1) \pm r_1 (Y_p - b_1) \sqrt{(X_p - a_1)^2 + (Y_p - b_1)^2 - r_1^2}}{(X_p - a_1)^2 + (Y_p - b_1)^2} + a_1 \quad [8]$$

$$Y_{t1,1}^{-} = Y_{t1,2}^{+} = \frac{r_1^2 (Y_p - b_1) \mp r_1 (X_p - a_1) \sqrt{(X_p - a_1)^2 + (Y_p - b_1)^2 - r_1^2}}{(X_p - a_1)^2 + (Y_p - b_1)^2} + b_1 \quad [9]$$

Once the tangent points have been identified for all rollers, the wrap angle (θ_i) can be determined. The wrap angle is defined as the sum of angles formed from the tangent point to either the top/bottom of the cylinder (whichever route the fibers take). For the case where roller

wrap angles are below 180° and the adjacent rollers remain in relative positions so the tangents are "logical", Equations 10 and 11 are valid. Some configurations would result in fibers crossing each other which is not possible in the actual process. Thus it is recommended to plot these points before proceeding to ensure the tangents that were defined are representative of the process layout. After determining the wrap angle, it is a simple exercise to relate the tension and wrap angle to the pressure generated moving over the roller.

$$\theta_0 = 90° - Tan^{-1}\left(\frac{X^-_{to,z} - X^-_{t1,z}}{Y^+_{to,z} - Y^+_{t1,z}}\right)\frac{180°}{\pi} \quad [10]$$

$$\theta_1 = 180° - Tan^{-1}\left(\frac{X^-_{to,z} - X^-_{t1,z}}{Y^+_{to,z} - Y^+_{t1,z}}\right)\frac{180°}{\pi} + Tan^{-1}\left(\frac{X^+_{t1,z} - X^+_{tz,z}}{Y^-_{tz,z} - Y^-_{tz,z}}\right)\frac{180°}{\pi} \quad [11]$$

2.4 Nip-Roll Impregnation Route for Hot-Melt

The Nip-Roll process utilizes 2 driven nip rollers, shown in Figure 3. The gap between the two rolls is set to a desired distance which serves as the thickness for the final prepreg. Thus this process is driven by displacement control. So the line speed will influence the degree of compaction and resin flow along with the physical gap distance. For modeling this system, the backing paper and resin are treated as a non-porous and incompressible material. While the fiber bed is considered to be a compressible, porous material. The porosity of the fiber bed and effective pressure is dependent on the compressed state of the fiber bed. The effective pressure is the pressure required to compress the fiber bed to the present fiber volume fraction.

Once the sandwich structure makes contact with the roller, a step wise integration of Darcy's Law can be used to predict the flow of resin in the fiber bed. At each time step, the fiber bed compresses to a new thickness, which is imposed by the distance between the roller at the position and the fiber bed mid plane. The new thickness can be related back to a fiber volume fraction. From fiber volume fraction the pressure and permeability are estimated. The flow velocity is calculated for each time step, and direct integration is not possible because pressure, viscosity, fiber volume fraction, and permeability are not constant. The resin film thickness is tracked as the material flows into the fiber bed.

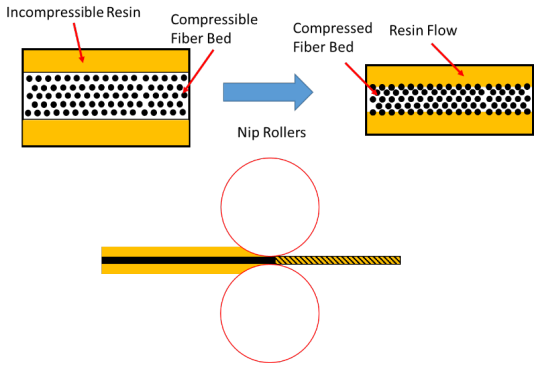

Figure 3: Example Hot-Melt process highlighting the compression of the fiber bed.

3. RESULTS

For this section, we will consider a Hot-Melt process where polyamide 6,6 (PA66) will be the polymer impregnating an aligned fiber bed composed of carbon fiber with a diameter of 7 μm. With the Hot-Melt process, the frictionless rollers in an S-Wrap will be considered for the first impregnation route. Then compare this impregnation route to the Nip-Roller process in terms of line operation.

An example S-wrap process was shown in Figure 1 with polyamide 6,6 polymer undergoing typical processing conditions. From the impregnation model, the resin infusion progress is linear and constant when pressure is applied, which is seen in Figure 4. This linear infusion behavior is a consequence of this process being force controlled. The tension in the line, wrap angle, and roller diameter are what dictate the driving force for resin flow. Under these conditions, inter-fiber spacing is predetermined and not expected to change significantly during processing across an individual roller.

The S-Wrap process spreads the impregnation step over a larger contact area on the roller. This reduces the speed of impregnation and fiber bed compaction. Conversely, the increased time in the process will advance the curing reaction for thermosets and degrade thermoplastics. Figure 4 shows the "dead time" between rollers for a notional roller configuration, where the resin is at an elevated temperature, the degradation is proceeding, and the impregnation is halted during this time. Additionally, the pulling force/tension will need careful monitoring so fiber breakage is avoided and impregnation can be tracked/compared to models. However, the avoidance of significant fiber bed compaction will reduce the likelihood of the particles suspended in the resin from being filtered by the fiber bed.

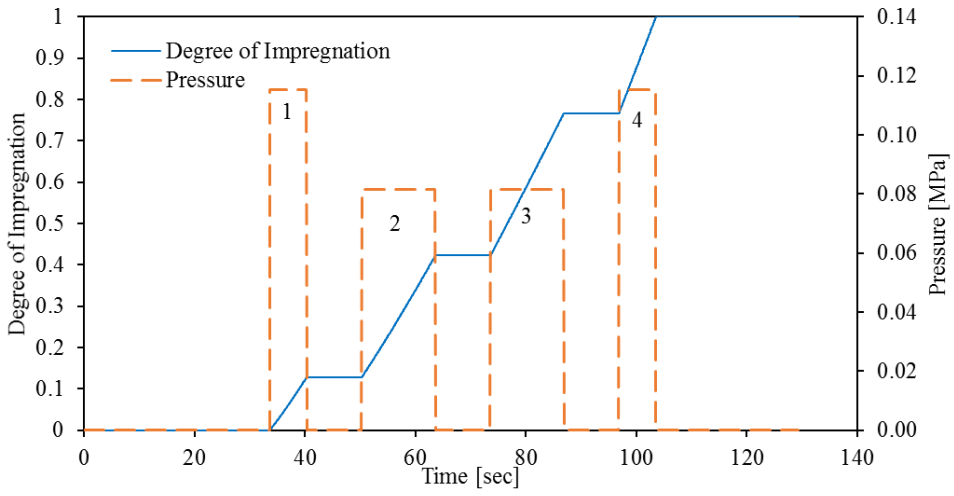

Figure 4: Tracking impregnation via S-Wrap with polyamide 6,6 resin for a line speed of 0.03 m/s, tension 7300 N, heated table length 1m, and heated table temperature 290 °C. Numbered peaks correspond to the numbering in Figure 1.

Unlike the S-Wrap process, Nip-Roll impregnation has variations in the impregnation velocity, which can be seen in Figure 5. The non-linear impregnation is caused by the change in

displacement rate as the material moves between the nip rollers. Since the displacement rate is a function of line speed, tuning line operations through trial and error becomes challenging as the non-linear pressure and permeability relationships are now linked to line speed. Additionally, there is significantly less contact time (~2 seconds) with the material and nip rollers than in the S-Wrap process. Which means greater pressure needs to be applied for the same line speed in order to achieve complete impregnation. Since the Nip-Roll process has greater pressure being applied, there is greater concern with the complete locking of the fiber bed. If line speeds are too fast, then material will be squeezed transversely out the sides of the process.

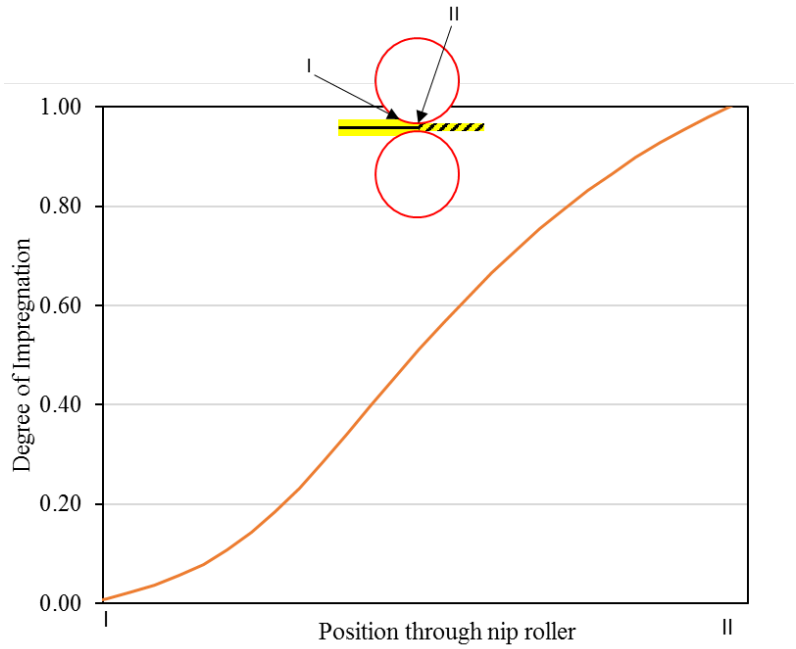

Figure 5: Predicted impregnation of PA 6,6 in a hot-melt process where point I is when the resin first makes contact with the nip roller and II is where prepreg loses contact with the nip roller. Line speed: 0.03 m/s. Material temperature: 290 °C. Heated table length 1m.

4. SUMMARY

In summary, there are many prepregging processes to choose from which are dependent on the chemistry of the polymer chosen for impregnation. In general, solvent/emulsion impregnation routes will reduce viscosity of the polymer and improve impregnation speeds. This method is used for viscous thermoplastic polymers. Other impregnations routes reduce impregnation distances. Some examples discussed were fiber commingling, film stacking, and powder deposition. Impregnation quality in these processes are dependent on the ability for the polymer to wet the fibers.

Finally, we considered a Hot-Melt impregnation process undergoing two different impregnation routes, S-wrap and Nip Roll. Modeling these processes showed by adjusting line tension or roller gap, complete impregnation can be achieved in both impregnation routes for the same line speed and temperature. However, the time material spent in the process was very different. S-Wrap impregnation spent 105 seconds compared to the 40 seconds for the Nip-Roll route. So greater

thermal degradation will occur in the S-Wrap process compared to the Nip-Roll. Since the impregnation time in the Nip-Roll route is significantly smaller, the applied pressure is greater so is the risk for fiber bed locking. Thus the S-Wrap process should be capable of achieving faster line speeds than the Nip-Roll process.

5. REFERENCES

[1] "Global Thermoplastic Composites Market Forecast to 2026: A $67.87 Billion Opportunity - ResearchAndMarkets.com." *Business Wire*, (2018), pp.

[2] Edwards, Tim. "Composite Materials Revolutionise Aerospace Engineering." *Ingenia*, no. 36, (2008), pp. 24-28.

[3] Barbosa, G. F. and J. Carvalho. "Analytical Model for Aircraft Design Based on Design for Excellence (Dfx) Concepts and Use of Composite Material Oriented to Automated Processes." *International Journal of Advanced Manufacturing Technology*, vol. 69, no. 9-12, (2013), pp. 2333-2342, doi:10.1007/s00170-013-5211-7.

[4] Martensson, P. et al. "Effects of Manufacturing Constraints on the Cost and Weight Efficiency of Integral and Differential Automotive Composite Structures." *Composite Structures*, vol. 134, (2015), pp. 572-578, doi:10.1016/j.compstruct.2015.08.115.

[5] *Code of Federal Regulations (Cfr) 2015, Title 40 - Protection of Environment, Parts 1 to 1899.* Office of the Federal Register OFR, (2015). *Code of Federal Regulations*.

[6] Gardiner, Ginger. "Composites in Class a Body Panels: Evolution Continues." Composites World, (2017).

[7] Favaloro, A. J. et al. "Simulation of Prepreg Platelet Compression Molding: Method and Orientation Validation." *Journal of Rheology*, vol. 62, no. 6, (2018), pp. 1443-1455, doi:10.1122/1.5044533.

[8] Lam, R. C. and J. L. Kardos. "The Permeability and Compressibility of Aligned and Cross-Plied Carbon-Fiber Beds During Processing of Composites." *Polymer Engineering and Science*, vol. 31, no. 14, (1991), pp. 1064-1070, doi:10.1002/pen.760311411.

[9] Gutowski, T. G. et al. "Consolidation Experiments for Laminate composites." *Journal of Composite Materials*, vol. 21, no. 7, (1987), pp. 650-669, doi:10.1177/002199838702100705.

[10] Sadiq, T. A. K. et al. "Experimental Investigation of Transverse flow-through Aligned Cylinders." *International Journal of Multiphase Flow*, vol. 21, no. 5, (1995), pp. 755-774, doi:10.1016/0301-9322(95)00026-t.

[11] Dave, R. et al. "A Model for Resin Flow During Composite processing .1. General Mathematical Development." *Polymer Composites*, vol. 8, no. 1, (1987), pp. 29-38, doi:10.1002/pc.750080106.

[12] Liu, B. et al. "Preparation of Carbon Fiber-Reinforced Thermoplastics with High Fiber Volume Fraction and High Heat-Resistant Properties." *Journal of Thermoplastic Composite Materials*, vol. 30, no. 5, (2017), pp. 724-737, doi:10.1177/0892705715610408.

[13] Patel, N. et al. "Micro Scale Flow Behavior and Void Formation mechanism During Impregnation through a Unidirectional Stitched Fiberglass Mat." *Polymer Engineering and Science*, vol. 35, no. 10, (1995), pp. 837-851, doi:10.1002/pen.760351006.

[14] Grunenfelder, L. K. et al. "Effect of Room-Temperature out-Time on Tow Impregnation in an out-of-Autoclave Prepreg." *Composites Part a-Applied Science and Manufacturing*, vol. 45, (2013), pp. 119-126, doi:10.1016/j.compositesa.2012.10.001.

[15] Betanzos, F. B. et al. "Cyclic Pressure on Compression-Moulded Bioresorbable Phosphate Glass Fibre Reinforced Composites." *Materials & Design*, vol. 100, (2016), pp. 141-150, doi:10.1016/j.matdes.2016.03.108.
[16] Gabrion, X. et al. "About the Thermomechanical Behaviour of a Carbon Fibre Reinforced High-Temperature Thermoplastic Composite." *Composites Part B-Engineering*, vol. 95, (2016), pp. 386-394, doi:10.1016/j.compositesb.2016.03.068.
[17] Gangloff, J. J. et al. "The Investigation of Bubble Mobility in Channel Flow with Wavy Porous Media Walls." *International Journal of Multiphase Flow*, vol. 70, (2015), pp. 1-14, doi:10.1016/j.ijmultiphaseflow.2014.11.005.
[18] Gangloff, J. J. et al. "Entrapment and Venting of Bubbles During Vacuum Bag Prepreg Processing." *Journal of Composite Materials*, vol. 51, no. 19, (2017), pp. 2757-2768, doi:10.1177/0021998316676325.
[19] Ramani, K. et al. "An Electrostatic Powder Spray Process for Manufacturing Thermoplastic Composites." *Polymer Composites*, vol. 16, no. 6, (1995), pp. 459-469, doi:10.1002/pc.750160604.
[20] Babeau, A. et al. "Modeling of Heat Transfer and Unsaturated Flow in Woven Fiber Reinforcements During Direct Injection-Pultrusion Process of Thermoplastic Composites." *Composites Part a-Applied Science and Manufacturing*, vol. 77, (2015), pp. 310-318, doi:10.1016/j.compositesa.2015.04.017.
[21] Borges, S. G. et al. "The Influence of Bath Temperature on the Properties of Pultruded Glass Fiber Reinforced Rods." *Journal of Reinforced Plastics and Composites*, vol. 34, no. 15, (2015), pp. 1221-1230, doi:10.1177/0731684415587411.
[22] Simacek, P. and S. G. Advani. "Simulating Tape Resin Infiltration During Thermoset Pultrusion Process." *Composites Part a-Applied Science and Manufacturing*, vol. 72, (2015), pp. 115-126, doi:10.1016/j.compositesa.2015.01.020.
[23] Irfan, M. S. et al. "A Modified Pultrusion Process." *Journal of Composite Materials*, vol. 51, no. 13, (2017), pp. 1925-1941, doi:10.1177/0021998316666653.
[24] Memon, A. and A. Nakai. "The Processing Design of Jute Spun Yarn/Pla Braided Composite by Pultrusion Molding." *Advances in Mechanical Engineering*, (2013), p. 8, doi:10.1155/2013/816513.
[25] Risicato, J. V. et al. "A Complex Shaped Reinforced Thermoplastic Composite Part Made of Commingled Yarns with Integrated Sensor." *Applied Composite Materials*, vol. 22, no. 1, (2015), pp. 81-98, doi:10.1007/s10443-014-9400-9.
[26] Grunenfelder, L. K. et al. "Effect of Room-Temperature out-Time on Tow Impregnation in an out-of-Autoclave Prepreg." *Composites Part a-Applied Science and Manufacturing*, vol. 45, (2013), pp. 119-126, doi:10.1016/j.compositesa.2012.10.001.
[27] Liker, Jeffrey K. *The Toyota Way : 14 Management Principles from the World's Greatest Manufacturer.* McGraw-Hill, (2004).
[28] Diez-Pascual, A. M. et al. "Poly(Phenylene Sulphide) and Poly(Ether Ether Ketone) Composites Reinforced with Single-Walled Carbon Nanotube Buckypaper: I - Structure, Thermal Stability and Crystallization Behaviour." *Composites Part a-Applied Science and Manufacturing*, vol. 43, no. 6, (2012), pp. 997-1006, doi:10.1016/j.compositesa.2011.11.002.
[29] Fang, X. et al. "Comparative Investigation of Molded Thickness and Surface Density on the Structures and Mechanical Properties of Lightweight Reinforced Thermoplastic

Composites." *Fibers and Polymers*, vol. 18, no. 2, (2017), pp. 303-312, doi:10.1007/s12221-017-6067-5.

[30] Sorrentino, L. et al. "Thermoplastic Composites Based on Poly(Ethylene 2,6-Naphthalate) and Basalt Woven Fabrics: Static and Dynamic Mechanical Properties." *Polymer Composites*, vol. 37, no. 8, (2016), pp. 2549-2556, doi:10.1002/pc.23449.

[31] Zhou, N. T. et al. "Mechanical and Sound Adsorption Properties of Cellular Poly (Lactic Acid) Matrix Composites Reinforced with 3d Ramie Fabrics Woven with Co-Wrapped Yarns." *Industrial Crops and Products*, vol. 56, (2014), pp. 1-8, doi:10.1016/j.indcrop.2014.02.029.

[32] Liu, B. et al. "Preparation of Carbon Fiber-Reinforced Thermoplastics with High Fiber Volume Fraction and High Heat-Resistant Properties." *Journal of Thermoplastic Composite Materials*, vol. 30, no. 5, (2017), pp. 724-737, doi:10.1177/0892705715610408.

[33] Xu, A. C. et al. "Molding of Pbo Fabric Reinforced Thermoplastic Composite to Achieve High Fiber Volume Fraction." *Polymer Composites*, vol. 34, no. 6, (2013), pp. 953-958, doi:10.1002/pc.22501.

[34] Connor, M. et al. "A Model for the Consolidation of Aligned thermoplastic Powder Impregnated Composites." *Journal of Thermoplastic Composite Materials*, vol. 8, no. 2, (1995), pp. 138-162.

[35] Connor, Marco. "Consolidation Mechanisms and Interfacial Phenomena in Thermoplastic Powder Impregnated Composites." (1995).

[36] Herceg, T. M. et al. "Thermosetting Hierarchical Composites with High Carbon Nanotube Loadings: En Route to High Performance." *Composites Science and Technology*, vol. 127, (2016), pp. 134-141, doi:10.1016/j.compscitech.2016.02.015.

[37] Dibenedetto, A. T. "Prediction of the Glass-Transition temperature of Polymers - a Model Based on the Principle of Corresponding states." *Journal of Polymer Science Part B-Polymer Physics*, vol. 25, no. 9, (1987), pp. 1949-1969, doi:10.1002/polb.1987.090250914.

[38] Ramis, X. and J. M. Salla. "Time-Temperature Transformation (Ttt) Cure Diagram of an Unsaturated Polyester Resin." *Journal of Polymer Science Part B-Polymer Physics*, vol. 35, no. 2, (1997), pp. 371-388, doi:10.1002/(sici)1099-0488(19970130)35:2<371::aid-polb13>3.3.co;2-6.

[39] Amico, S. and C. Lekakou. "An Experimental Study of the Permeability and Capillary Pressure in Resin-Transfer Moulding." *Composites Science and Technology*, vol. 61, no. 13, (2001), pp. 1945-1959, doi:10.1016/s0266-3538(01)00104-x.

[40] Reichanadter, Alex et al. "Process Modeling and Flexible Manufacturing of Multi-Phase Resin Based Thermoset and Thermoplastic Prepreg." SPE-ACCE Conference, (2018).

[41] Astrom, B. T. et al. "On Flow through Aligned Fiber Beds and Its Application to Composites Processing." *Journal of Composite Materials*, vol. 26, no. 9, (1992), pp. 1351-1373, doi:10.1177/002199839202600907.

[42] AmBrSoft. "Tangent lines between two circles," (2017).